

Pruning the Way to Reliable Policies: A Multi-Objective Deep Q-Learning Approach to Critical Care

Ali Shirali*¹, Alexander Schubert*¹, and Ahmed Alaa¹

¹University of California, Berkeley

Abstract

Most medical treatment decisions are sequential in nature. Hence, there is substantial hope that reinforcement learning may make it possible to formulate precise data-driven treatment plans. However, a key challenge for most applications in this field is the sparse nature of primarily mortality-based reward functions, leading to decreased stability of offline estimates. In this work, we introduce a deep Q-learning approach able to obtain more reliable critical care policies. This method integrates relevant but noisy intermediate biomarker signals into the reward specification, without compromising the optimization of the main outcome of interest (e.g. patient survival). We achieve this by first pruning the action set based on all available rewards, and second training a final model based on the sparse main reward but with a restricted action set. By disentangling accurate and approximated rewards through action pruning, potential distortions of the main objective are minimized, all while enabling the extraction of valuable information from intermediate signals that can guide the learning process. We evaluate our method in both off-policy and offline settings using simulated environments and real health records of patients in intensive care units. Our empirical results indicate that pruning significantly reduces the size of the action space while staying mostly consistent with the actions taken by physicians, outperforming the current state-of-the-art offline reinforcement learning method conservative Q-learning. Our work is a step towards developing reliable policies by effectively harnessing the wealth of available information in data-intensive critical care environments.

1 Introduction

Specifying a reward function poses a challenge in many (applied) reinforcement learning (RL) settings. In the presence of multiple desirable factors, it is often unclear how to obtain a single scalar reward. Additionally, even when a single outcome is of interest, it may be too rare to learn from directly with limited data. To address this issue, less accurate but more frequent reward proxies can be incorporated. However, if these proxies are included in the reward specification without sufficient consideration, the resulting policy may deviate from optimizing the true reward.

This challenge frequently arises in the medical context where RL’s promise is to obtain personalized treatment policies. Many medical decisions require physicians to periodically select among multiple treatments or to prescribe the right diagnostic tests at the right time. The sequential nature of these problems and the increasing availability of health data make it a potential use case of RL. In many settings, patient survival is a critical outcome of interest, but it is a rare event that only provides a delayed and sparse signal. As an alternative, medical risk scores can be used as more frequent intermediate rewards. However, these scores are only approximations of a patient’s true individualized severity and may be biased for certain populations (Miller et al., 2021). Hence, determining the most effective way to integrate information from these intermediate signals into RL policies still remains a challenge.

In recent years, there has been a surge of interest in exploring the prospects of RL in critical care settings (Henry et al., 2015; Prasad et al., 2017; Raghu, Komorowski, Celi, et al., 2017; Raghu, Komorowski, and Singh, 2018; Cheng, Prasad, and Barbara E. Engelhardt, 2018b; Komorowski et al., 2018; Lin et al.,

*Equal contribution

2018; Peine et al., 2021; Fatemi, Killian, et al., 2021). Different studies have taken different approaches towards defining the reward function. For instance, focusing on the task of managing vasopressor and intravenous fluids in sepsis patients, Komorowski et al. (2018) solely reward the agent based on 90-day survival, while Raghu, Komorowski, Celi, et al. (2017) have further included intermediate rewards based on the SOFA-score (Vincent et al., 1996) and arterial lactate levels.

As mentioned earlier, directly incorporating more frequent but less accurate intermediate reward signals comes at a cost. Distortions from these rewards can cause the final policy to deviate from the primary outcome of interest. Furthermore, the varying complexity in the structures of different rewards can pose unique learning challenges for an RL agent. As a result, there is a risk that the agent could primarily optimize toward rewards that are easier to learn, inadvertently neglecting the genuine, more complex outcomes of interest.

In order to overcome this challenge, we propose a new two-stage algorithm that partially disentangles learning from inaccurate intermediate rewards and the sparse reward of interest. In the first stage, we propose a multi-objective Q-learning algorithm that enables us to *prune* the action set based on all available rewards without committing to an explicit relationship between them. Pruning is a relaxed version of a policy, that instead of prescribing a single action to take, removes unpromising actions which are unlikely to make any improvement to any linearly scalarized reward. This relaxation will minimize the possible distortion due to less accurate rewards while guiding the second stage where we run standard Q-learning on the pruned action set.

We evaluate our framework in both off-policy and offline settings using simulated environments and real data. In the off-policy setting of OpenAI Gym Lunar Lander environment (Brockman et al., 2016), we show that our algorithm can effectively prune the action space and that this reduction in complexity significantly improves learning based on the sparse reward later on.

We further evaluate our framework in an offline setting using real health records of septic patients in the intensive care unit (ICU). We demonstrate that simply linearly combining rewards does not effectively improve standard Q-learning. However, by using our two-stage algorithm, medical scores can effectively enhance the policy outcome. Additionally, we find that the pruning step significantly reduces the number of available actions without discarding the actions chosen by physicians in the majority of cases.

A desirable characteristic of a reliable offline RL policy is to adhere to the expert policy, in this case, the physician policy, as closely as possible while incurring minimal performance losses compared to an unrestricted policy. Conservative Q-learning (CQL) (Kumar et al., 2020) is a prevalent method used to enforce such similarity. Our results demonstrate that our method achieves a high similarity to physician actions comparable with CQL while attaining superior performance. This indicates that our approach is promising in obtaining relevant offline policies while avoiding out-of-distribution actions.

Reinforcement learning holds the promise of deriving personalized treatment policies in healthcare that cater to the unique history of each patient. However, achieving this requires models that can effectively assimilate information from diverse inputs, while also being able to accurately distinguish between key outcomes and potentially biased or less accurate proxies. Our work presents a new approach that takes us closer to achieving this goal. Our two-stage algorithm allows us to effectively integrate information from intermediate severity proxies, resulting in better performance compared to standard conservative Q-learning methods. This is particularly important in critical care processes, where intermediate indicators are abundant, and it is crucial that computational methods can accurately respond to these signals when providing recommendations.

The code to derive the presented results is available at:

<https://github.com/alishiraliGit/multi-criteria-deep-q-learning>

2 Related Work

Multi-Objective Reinforcement Learning. The main body of work on multi-objective (or multi-criteria) reinforcement learning (RL) can be divided into single-policy methods and multiple-policy methods. We refer the reader to C. Liu, X. Xu, and Hu (2015) for a survey of the field. Single-policy methods (Mannor and Shimkin, 2001; Tesauro et al., 2007) reduce multiple objectives into a single scalar reward assuming a known user-specified or context-driven preference over different objectives and then seek to maximize the

scalarized objective using standard RL techniques. The major difference between different single-policy approaches lies in the way in which they attempt to derive preferences over objectives. These methods, however, cannot be used when the preferences themselves are unknown.

In contrast, multi-policy methods aim to estimate the Pareto frontier based on a set of policies. One way to achieve this is by training an ensemble of policies based on different reward scalarizations (Natarajan and Tadepalli, 2005; Van Moffaert, Drugan, and Nowe, 2013; Mossalam et al., 2016; Cheng, Prasad, and Barbara E Engelhardt, 2018a; J. Xu et al., 2020). These methods require exhaustive training and in some cases non-trivial scalarizations. Other methods extend the standard scalar variables in RL algorithms to vector variables and use updating rules in the vector space. Most related to our proposed method of multi-objective Q-learning (Section 4.1) are such value-based methods. Early work in this direction explored the problem of acquiring all Pareto optimal policies simultaneously (Barrett and Narayanan, 2008; Hiraoka, Yoshida, and Mishima, 2008; Iima and Kuroe, 2014). Their methods focused on applications in online settings and on small, finite-state spaces. Lizotte and Laber (2016) extended Barrett and Narayanan (2008)’s framework to real-valued state features but with an exponential complexity in time horizon and in the size of the action space. In contrast, our deep Q-learning method runs for arbitrarily long trajectories in polynomial time by using an approximate problem formulation. Furthermore, our familiar formulation enables our method to leverage the recent advances in offline Q-learning.

Overall, a key focus of this research area lies in either inferring optimal preference weights or directly uncovering a set of Pareto-optimal policies. Instead, to the best of our knowledge, this study is the first to leverage multi-objective RL to prune the action space by identifying and eliminating inferior state-actions pairs in order to reduce the complexity of the learning problem for subsequent learning tasks.

Non-Deterministic Policies. While the mathematical framework we employ to devise a pruning function in phase 1 of our algorithm echoes certain aspects of the research on non-deterministic policies (or set-valued policies) (Fard and Pineau, 2011; Tang, Modi, M. Sjoding, et al., 2020), our methodology diverges in various ways. Firstly, non-deterministic policies sacrifice performance to provide a set of potential solutions instead of a single distinct action. In contrast, our method intends to improve policy performance. This is achieved as it combines a set-valued policy formulation to prune the action space in phase 1, allowing for more effective policies in phase 2. While non-deterministic policies remain prescriptive, this way our pruning function largely acts as a prohibitive measure that eliminates suboptimal choices from the action set.

Reinforcement Learning in Health. In recent years, RL has been the focus of several studies in health-care. See (S. Liu et al., 2020) for a review. There has been a particular focus on personalized treatment plans for sepsis patients in the ICU (Henry et al., 2015; Futoma et al., 2017; Raghu, Komorowski, Celi, et al., 2017; Komorowski et al., 2018; Saria, 2018; Peng et al., 2018; Tang, Modi, M. W. Sjoding, et al., 2020; Raghu, Komorowski, and Singh, 2018). However, these studies either leverage sparse mortality information alone to assign rewards or combine multiple intermediate sepsis risk proxies based on a deterministic weight. To the best of our knowledge, our approach is the first attempt to explicitly address the challenges imposed by sparse rewards in this context by proposing to prune the action space before estimating a final policy.

Dead-End State Identification. Given the focus of the pruning stage of our algorithm on eliminating dominated actions, our method is related to work on dead-end identification in RL (Irpan et al., 2018; Fatemi, Sharma, et al., 2019; Fatemi, Killian, et al., 2021). For instance, Fatemi, Killian, et al. (2021) developed an RL algorithm to identify and avoid “medical dead-end” states, defined as states from which no action can be made to achieve a positive terminal outcome (e.g. survival). While the aim of this method is conceptually close to the goal of our pruning stage, we propose a distinct technical approach to achieve this goal. Fatemi, Killian, et al. (2021)’s work focuses on classifying states that should be avoided; in contrast, our method directly identifies and excludes dominated state-action pairs. Furthermore, our method does not stop at the identification of risky actions but instead leverages the pruned action space for the subsequent training of an optimal policy.

3 Notation and Preliminaries

Reinforcement Learning. Following the terminology commonly adopted in the area of RL, we imagine an agent interacting with an environment. As the agent executes an *action*, denoted as $a \in \mathcal{A}$, in a given *state*, denoted as $s \in \mathcal{S}$, a *reward*, expressed as $r(s, a)$, materializes, and the environment’s state subsequently updates to s' . The agent can then utilize this reward as feedback to make more optimal future action choices. The agent’s decision-making process is often elucidated through a *policy*. In general, a policy $\pi : \mathcal{S} \rightarrow \Delta(\mathcal{A})$ provides a distribution over potential actions for each state. A deterministic policy $\pi : \mathcal{S} \rightarrow \mathcal{A}$ singles out a specific action given the current state. Our study particularly focuses on *offline* RL, where the aim is to devise an effective policy based on previously collected data. Simultaneously, our algorithms are also applicable in *off-policy* settings where the agent interacts with the environment at selected time steps. We denote the available data as a set of transitions \mathcal{D} . Each transition is a tuple (s, a, s', r) demonstrating that at state s , the action a is taken, which resulted in a state transition to s' and a reward of r .

Q-Learning. A standard (scalar) *Q-function* $Q^\pi : \mathcal{S} \times \mathcal{A} \rightarrow \mathbb{R}$ estimates the value of policy π at state s given that the agent takes action a at s and follows policy π thereafter. This value signifies a discounted sum of rewards, with any rewards realized at a later timestep being discounted by a factor of γ . At times, we omit the superscript π as our focus is on the optimal policy. The deep learning structure that implements the Q-function is occasionally referred to as a *Q-network*. We use the terms Q-function and Q-network interchangeably. In the context of Q-Learning, we sample a batch of transitions $\mathcal{B} \in \mathcal{D}$ and employ the Bellman equation to update the Q-network:

$$Q(s, a) \leftarrow r + \gamma \max_{a'} Q(s', a'). \tag{1}$$

Let the Q-network be parameterized by θ . Then the above notation is a shorthand to update θ from its current value θ_0 by minimizing the loss

$$\mathcal{L}(\theta) = \sum_{(s,a,s',r) \in \mathcal{B}} (Q_\theta(s, a) - r - \gamma \max_{a'} Q_{\theta_0}(s', a'))^2. \tag{2}$$

Commonly, we implement this update via a single or a couple of gradient descent steps. However, Q-learning based on the above formulation suffers from a fast-moving target and overestimation. These challenges can be addressed by employing a target network Q' along with an update rule, recognized as double Q-learning (Van Hasselt, Guez, and Silver, 2016):

$$Q(s, a) \leftarrow r + \gamma Q'(s', \arg \max_{a'} Q(s', a')). \tag{3}$$

In the context of double Q-learning, the target network Q' is updated by $Q' \leftarrow Q$ after hundreds or thousands of updates to Q . The final deterministic policy is then extracted as $\pi(s; Q) = \arg \max_a Q(s, a)$.

(Suboptimal) Q-Learning With Softmax Policies. In the original Bellman equation, the optimal policy is greedy and deterministic with respect to the Q-values, achieved through the use of the arg max function to locate the most effective action. However, empirical evidence has shown that applying a softmax operator tends to yield superior policies, particularly in the context of deep Q-networks. This relaxation has also garnered recent theoretical support (Song, Parr, and Carin, 2019). Formally, given a Q-function Q , we can derive a stochastic softmax policy π^β as

$$\pi^\beta(a|s; Q) = \frac{\exp(\beta Q(s, a))}{\sum_{\bar{a}} \exp(\beta Q(s, \bar{a}))}, \tag{4}$$

where β is an inverse temperature parameter. Note that in the limit of $\beta \rightarrow \infty$, the softmax policy converges to a deterministic arg max policy. Let us define

$$\text{softmax}_{a'} Q(s', a') := \sum_{a'} \pi^\beta(a'|s'; Q) Q(s', a'). \tag{5}$$

We dropped the dependence on π^β from the softmax notation for convenience. Note that $\text{softmax}_{a'} Q(s', a') \rightarrow \max_{a'} Q(s', a')$ as $\beta \rightarrow \infty$. A Bellman update using softmax can then be obtained by substituting the max with a softmax operator in Equation 1. Similarly, we can implement double Q-learning using a softmax policy:

$$Q(s, a) \leftarrow r + \gamma \sum_{a'} \pi^\beta(a'|s'; Q) Q'(s', a'). \quad (6)$$

Vector-Valued Reward and Q-Function. In many practical scenarios, the reward from an interaction can have multiple dimensions. For example, consider the case where there is a sparse main reward r_* as well as a set of noisy but more frequent rewards. In these cases, we gather all the rewards into a *vector reward* $\mathbf{r} \in \mathbb{R}^d$ and use r_i to refer to the i^{th} reward. We introduce a *vector-valued Q-function* $\mathbf{Q} : \mathcal{S} \times \mathcal{A} \rightarrow \mathbb{R}^d$ which for any state-action pair outputs a vector of estimated values. Q_i denotes the i^{th} dimension of \mathbf{Q} that encodes the value from r_i . We discuss learning vector-valued Q-functions in Section 4.1.

4 Methods

The main objective of this study is to formulate an approach that facilitates the efficient incorporation of frequent yet imprecise reward signals while preventing such signals from causing the policy to diverge from maximizing the primary sparse reward of interest. We hypothesize that while some biomarkers or clinical risk scores might be too noisy to be directly used in deriving an optimal policy they may still be useful to *identify actions to avoid*. Hence, we propose a two-stage algorithm: In the first phase, we learn a vector-valued Q-function relying on (noisy) intermediate rewards. This Q-function will be the basis to *prune* the action set at each state. Then in the second phase, we search for the optimal policy based on the (accurate) sparse reward. Actions dropped in the first phase won't be available to the policy of the second phase, which reduces the complexity of the learning problem and thus facilitates learning from the sparse reward.

4.1 Phase 1: Multi-Objective Deep Q-Learning

In this section, we first review direct ways to incorporate noisy intermediate reward signals into a reinforcement learning objective through explicit scalarization and discuss why this is challenging in our setting. We then motivate and propose a vector-valued Q-learning algorithm that avoids any explicit scalarization. We later augment our method for the offline setting by applying techniques from conservative Q-learning. We conclude the description of phase 1 by developing a stochastic policy based on the trained vector-valued Q-function.

Challenges of Single-Policy Methods. A direct method to combine a sparse main reward and intermediate reward signals is through scalarization of the reward vector \mathbf{r} . In the multi-objective RL literature, this approach is generally referred to as single-policy methods. In its simplest form, consider a linearly weighted combination $\mathbf{w}^\top \mathbf{r}$ where $\mathbf{w} \in \mathbb{R}^d$ determines the relative importance of each reward aspect. We assume $w_i \geq 0$ and $\sum_{i=1}^d w_i = 1$. Leveraging the combined reward as the standard Q-learning objective, we can then obtain the Q-function $Q^{\mathbf{w}}$ and its corresponding (possibly stochastic) policy $\pi^\beta(\cdot|\cdot; Q^{\mathbf{w}})$. However, this approach comes with multiple challenges: First, we might not have knowledge of the best \mathbf{w} a priori. The selection of the weighting \mathbf{w} entails a trade-off between the smoothness of learning and the accuracy of approximating the main reward. The stronger a frequent intermediate reward is represented in the combined reward, the smoother the learning. But as the intermediate rewards carry a high level of noise, the final policy might deviate from maximizing r_* in an unwanted way. Second, a good \mathbf{w} to integrate the noisy intermediate reward signals might not exist at all. In fact, to facilitate learning, intermediate rewards should be present in the scalarized version with a minimal power. At this point, the signal from intermediate signals might be so strong that the Q-network mainly exploits the easy-to-learn intermediate rewards. Our experiments in the context of treating sepsis in an ICU setting suggest that such direct incorporation of intermediate reward signals into the objective leads to a deterioration of policy performance compared to a policy trained based on the sparse reward alone.

Challenges of Multi-Policy Methods With Ensemble of Policies. One way to get around the challenges of committing to a single weighting \mathbf{w} of rewards is to consider a set of weightings and obtain an ensemble of policies. Although this method does not obtain a single policy, it can still prune the action set at each state by removing the actions not prescribed by any policy in the ensemble. The possibility of having multiple weightings address our uncertainty about the best weighting but there remain multiple challenges: First, as mentioned previously, there might not be a good \mathbf{w} at all. In this case, policies in the ensemble are either unstable if their corresponding \mathbf{w} is heavily concentrated on the true sparse reward r_* or they are largely affected by noisy intermediate rewards. Second, training a comprehensive ensemble of models for a high-dimensional reward space is computationally expensive. To address these problems, we follow Barrett and Narayanan (2008) and Lizotte and Laber (2016) and suggest a vector-valued Q-learning approach that simultaneously learns optimal policies for several weightings of interest.

A Vector-Valued Q-Learning Approach. Given the aforementioned challenges of incorporating intermediate rewards through explicit scalarization, we present a Q-learning approach to obtain a vector-valued Q-function \mathbf{Q} . We aim to obtain a vector-valued Q-function such that $Q^{\mathbf{w}}(s, a) \approx \mathbf{w}^\top \mathbf{Q}(s, a)$ for almost every $\mathbf{w} \in \mathcal{W}$. Such a Q-function addresses the previously mentioned challenges as it does not commit to any explicit \mathbf{w} when incorporating intermediate rewards into learning and will subsequently be at the heart of our action-pruning approach in phase 2. In the following, we first show that a naive extension of the Bellman update to vector-valued Q-networks does not allow us to derive a universal update rule. Hence, to obtain a vector-valued Bellman update in the familiar form of Equation 1, we relax the problem in two ways: First, instead of estimating exact Q-functions, we conservatively approximate them. We show that our approximation may only underestimate values from actions unlikely to be taken by any optimal policy, and thus should have a minimal effect on performance. Second, we limit the weightings of interest by considering a prior \mathcal{P} over \mathcal{W} . A good prior should be both inclusive and spread-out. It should assign enough weight to the true reward, ensuring its presence in the pruning policy with a non-negligible probability, while avoiding concentration that leads to the same problems as fixing a specific \mathbf{w} .

First, to show that a naive extension of the Bellman update of $Q^{\mathbf{w}}$ cannot provide a universal updating rule for \mathbf{Q} , consider a fixed \mathbf{w} and rewrite the Bellman update of $Q^{\mathbf{w}}$ assuming $Q^{\mathbf{w}}(s, a) = \mathbf{w}^\top \mathbf{Q}(s, a)$:

$$\mathbf{w}^\top \mathbf{Q}(s, a) \leftarrow \mathbf{w}^\top \mathbf{r} + \gamma \operatorname{softmax}_{a'} \mathbf{w}^\top \mathbf{Q}(s', a'). \quad (7)$$

The above update depends on \mathbf{w} and in general, cannot be true for every $\mathbf{w} \in \mathcal{W}$. To observe this, note that the left-hand side of Equation 7 is linear in \mathbf{w} , but the right-hand side is not.¹

To make the update of Equation 7 universally true for every \mathbf{w} , we propose a linear conservative approximation:

$$\operatorname{softmax}_{a'} \mathbf{w}^\top \mathbf{Q}(s', a') \approx \sum_{a'} \pi^\beta(a'|s'; \hat{\mathbf{w}}^\top \mathbf{Q}) \mathbf{w}^\top \mathbf{Q}(s', a'), \quad (8)$$

where $\hat{\mathbf{w}} \sim \mathcal{P}$. To see that this approximation is conservative for any $\hat{\mathbf{w}}$, note that for large values of β , π^β converges to a deterministic policy which chooses $\hat{a} = \arg \max_{a'} \hat{\mathbf{w}}^\top \mathbf{Q}(s', a')$ and we have

$$\operatorname{softmax}_{a'} \mathbf{w}^\top \mathbf{Q}(s', a') \rightarrow \max_{a'} \mathbf{w}^\top \mathbf{Q}(s', a') \geq \mathbf{w}^\top \mathbf{Q}(s', \hat{a}). \quad (9)$$

Using the approximation in Equation 8, both sides of Equation 7 become linear in \mathbf{w} and we can thus derive a vector update for \mathbf{Q} independent of \mathbf{w} :

$$\mathbf{Q}(s, a) \leftarrow \mathbf{r} + \gamma \sum_{a'} \pi^\beta(a'|s'; \hat{\mathbf{w}}^\top \mathbf{Q}) \mathbf{Q}(s', a'). \quad (10)$$

The approximation of Equation 8 can be loose for a specific \mathbf{w} if the optimal action for $\hat{\mathbf{w}}$ at state s' diverges significantly from the optimal action for \mathbf{w} . We address this potential issue in the following manner. First, we consider a prior \mathcal{P} over \mathcal{W} . This prior can rule out implausible weightings. Second, when considering a fixed \mathbf{w} , if $\pi^\beta(a|s; \mathbf{w}^\top \mathbf{Q}) \ll 1$, we do not need to worry about the approximation being inaccurate as it most likely underestimates the value of an action unlikely to be taken. Conversely, if $\pi^\beta(a|s; \mathbf{w}^\top \mathbf{Q})$ is substantial,

¹In the case of deterministic policies, the right-hand side will be piecewise linear.

we desire a tight approximation. Hence, we only require $\hat{\mathbf{w}}$ to be a close approximation for a \mathbf{w} that results in the selection of action a at state s . Formally, given the prior \mathcal{P} and the observation that action a is taken at state s , we can procure a posterior over \mathcal{W} :

$$\mathcal{P}(\mathbf{w}|s, a) \sim \mathcal{P}(\mathbf{w}) \pi^\beta(a|s; \mathbf{w}^\top \mathbf{Q}). \quad (11)$$

We then draw $\hat{\mathbf{w}}$ from this posterior. Any posterior sampling method can be used here. For simplicity, we use a one-iteration of particle filtering which is essentially sampling particles from \mathcal{P} , reweighting them according to π^β , normalizing the weights, and then resampling.

To further improve the stability and performance of the algorithm, we use double-Q learning (Van Hasselt, Guez, and Silver, 2016) by introducing another vector-valued Q-network \mathbf{Q}' as the target network. The target network \mathbf{Q}' is updated after multiple updates of \mathbf{Q} by copying the weights from \mathbf{Q} . Our update rule for \mathbf{Q} is:

$$\mathbf{Q}(s, a) \leftarrow \mathbf{r} + \gamma \sum_{a'} \pi^\beta(a'|s'; \hat{\mathbf{w}}^\top \mathbf{Q}) \mathbf{Q}'(s', a'), \quad (12)$$

where we draw $\hat{\mathbf{w}}$ from posterior $\mathcal{P}(\cdot|s, a)$. We will refer to this method as *multi-objective Q-learning (MQL)* in the following sections.

Applying Techniques From Conservative Q-Learning. Offline Q-learning is prone to overestimating Q-values for states and actions not present in the dataset. Conservative Q-learning (CQL) has been proposed to mitigate this issue (Kumar et al., 2020). CQL seeks to prevent the overestimation of Q-values for out-of-distribution (s, a) pairs by enforcing a conservative loss function. Note that our proposed approximate update rule of Equation 12 is already conservative. However, we can further increase its conservativeness towards actions that are already present in the data by applying a technique similar to CQL. Specifically, let \mathbf{Q} be parameterized by θ . We use an augmented loss function

$$\mathcal{L}_\alpha(\theta; (s, a, s', \mathbf{r})) = \mathcal{L}(\theta; (s, a, s', \mathbf{r})) + \frac{\alpha}{d} \sum_{i \in [d]} \left[\log \left(\sum_{\bar{a}} \exp Q_{i, \theta}(s, \bar{a}) \right) - Q_{i, \theta}(s, a) \right], \quad (13)$$

where $\mathcal{L}(\theta; (s, a, s', \mathbf{r}))$ is the loss from the updating rule of Equation 12:

$$\mathcal{L}(\theta; (s, a, s', \mathbf{r})) = \left\| \mathbf{Q}_\theta(s, a) - \mathbf{r} - \gamma \sum_{a'} \pi^\beta(a'|s'; \hat{\mathbf{w}}^\top \mathbf{Q}) \mathbf{Q}'(s', a') \right\|_2^2. \quad (14)$$

For a sampled batch of data \mathcal{B} , the overall loss thus becomes:

$$\mathcal{L}_\alpha = \sum_{(s, a, s', \mathbf{r}) \in \mathcal{B}} \mathcal{L}_\alpha(\theta; (s, a, s', \mathbf{r})). \quad (15)$$

We will refer to this method as *multi-objective conservative Q-learning (MCQL)*.

A Stochastic Policy Out of Vector-Valued Q-Function. Neither MQL nor MCQL requires obtaining an explicit policy from \mathbf{Q} to be trained in the offline setting. However, in the off-policy setting, the agent interacts with the environment and therefore requires to have a policy at different points during training. We can define a stochastic policy based on \mathbf{Q} for a prior \mathcal{P} over weightings as

$$\pi_{\mathcal{P}}^\beta(a|s) := \mathbb{E}_{\mathbf{w} \sim \mathcal{P}} [\pi^\beta(a|s; \mathbf{w}^\top \mathbf{Q})]. \quad (16)$$

In practice, the agent interacts with the environment by sampling from $\pi_{\mathcal{P}}^\beta$ in two steps:

1. Draw $\mathbf{w} \sim \mathcal{P}$.
2. Draw $a \sim \pi^\beta(\cdot|s; \mathbf{w}^\top \mathbf{Q})$.

The importance of $\pi_{\mathcal{P}}^\beta$ extends beyond the off-policy setting as we will use it to prune actions at each state in the next section.

4.2 Phase 2: Q-Learning with Pruning

The new notion of stochastic policy $\pi_{\mathcal{P}}^{\beta}$ in Equation 16 can be interpreted as a relaxation to the notion of policy with explicit dependence on a specific \mathbf{w} . An important property of $\pi_{\mathcal{P}}^{\beta}$ is its inclusiveness, meaning that as long as the accurate reward r_* is sufficiently strongly represented in some \mathbf{w} with a noteworthy measure, the action maximizing r_* will be present in $\pi_{\mathcal{P}}^{\beta}$ with a non-negligible probability. Therefore, a reasonable way to prune the action set is to drop actions with $\pi_{\mathcal{P}}^{\beta}(a|s)$ below a threshold. But calculating $\pi_{\mathcal{P}}^{\beta}(a|s)$ requires a posterior calculation that can be computationally hard. Thus, we propose the following pruning function $\Pi^{\beta} : \mathcal{S} \rightarrow 2^{\mathcal{A}}$ by sampling from $\pi_{\mathcal{P}}^{\beta}$:

1. At state s , draw m actions $a^{(k)} \sim \pi_{\mathcal{P}}^{\beta}(\cdot|s)$ for $k \in [m]$:
 - (a) Draw m samples $\mathbf{w}^{(k)} \sim \mathcal{P}$ for $k \in [m]$.
 - (b) For each $\mathbf{w}^{(k)}$, draw $a^{(k)} \sim \pi^{\beta}(\cdot|s; \mathbf{w}^{(k)\top} \mathbf{Q})$.
2. Set $\Pi^{\beta}(s) = \{a^{(k)} \mid k \in [m]\}$.

The choice of m and β determines the expected size of the set $\Pi^{\beta}(s)$. As a rule of thumb, actions with $\pi_{\mathcal{P}}^{\beta}(a|s) < 1/m$ are unlikely to remain in the action set after pruning. In practice, we fix m to at least three times $|\mathcal{A}|$ to make sure that all actions have the chance to be in $\Pi^{\beta}(s)$ but very rare actions do usually not appear. Then tuning the value of β allows us to control pruning strictness as larger values move the policy closer to a deterministic policy. We treat β as a hyperparameter.

For a choice of β we then run standard double-Q learning using only the sparse main reward and restricting the action set to the actions chosen by pruning function Π^{β} . In doing so, we revisit Equation 3:

$$Q(s, a) \leftarrow r + \gamma Q'(s', \arg \max_{a' \in \Pi^{\beta}(s')} Q(s', a')). \tag{17}$$

It is worth noting that a similar modification of the loss function as in our discussion of conservative Q-learning (Kumar et al., 2020) yields a conservative version of Q-learning with pruning.

Examining Equation 17, we observe that $\Pi^{\beta}(s')$ is the only place where we incorporate noisy intermediate reward signals. Consequently, our final policy focuses solely on optimizing the accurate reward, ensuring that the original objective remains unaltered. We claim that the disentanglement of noisy and accurate rewards through this two-stage algorithm enables us to effectively incorporate information from intermediate signals to simplify the learning problem while minimally manipulating the policy’s true objective.

We refer to the two-stage algorithm presented in this paper as *Pruned QL*, which consists of MQL in the first phase and Q-learning with pruning in the second phase. In the offline setting, we call the conservative version consisting of MCQL in the first phase and CQL with pruning in the second phase, *Pruned CQL*.

5 Results

We first present the capability of our method within the OpenAI Gym Lunar Lander environment (Brockman et al., 2016), which provides the advantage of allowing us to observe the performance of the learned policy when rolled out. Subsequently, we evaluate our framework in an offline setting using real health records of septic patients in the intensive care unit (ICU) obtained from the MIMIC (Medical Information Mart for Intensive Care)-III dataset (v1.4) (Johnson et al., 2016).

5.1 Synthetic Experiments on Lunar Lander

We briefly demonstrate the prospects of our action space pruning approach using the game Lunar Lander. In Lunar Lander, the objective is to successfully land a small spaceship on the moon. In addition to the ultimate goal, three intermediate rewards related to the shape and fuel efficiency of the lander are also available, which can guide the landing process. The availability of a sparse main objective and informative intermediate signals makes Lunar Lander an appropriate choice for evaluating our proposed approach.

In particular, we conduct two experiments. First, we examine whether incorporating intermediate signals through action pruning is effective. To do so, we train a (double) Q-learning baseline model² on the sparse reward and compare it to our Pruned QL method. Please refer to the note at the end of this section for the model parameters. Figure 1(a) shows the development of the policy best returns as we interact more with the environment. After 500,000 iterations the baseline method struggles to learn a good policy solely based on the sparse reward and yields an average return of -70 close to the minimum of -100 . In contrast, our Pruned QL approach, which also only leverages sparse rewards in its final learning phase, achieves a substantially higher best return of around 50 within a shorter time. These results hold for varying pruning strengths β . It is important to note that Pruned QL benefits from additional reward signals during its first stage of MQL, making a direct comparison with the baseline not entirely fair. Nonetheless, these results are promising in that they underscore the potential of MQL-based action space pruning.

We next demonstrate how Pruned QL behaves as the intermediate reward signal becomes less precise. To achieve this we conduct a second experiment where we add white noise with standard deviations of 0.1, 1, and 10 to the intermediate rewards. Figure 1(b) depicts the results. We observe that Pruned QL remains robust until raising the white noise standard deviation to 10, where it only does marginally better than the baseline. This result illustrates two important characteristics of our method. First, it shows that Pruned QL has generally high robustness to noise. Second, the fact that the performance drops when the noise standard deviation is increased to 10 indicates that the intermediate rewards considered in this method must carry some relevant information about the sparse outcome of interest. At a white noise standard deviation of 10, the signal-to-noise ratio (SNR) of the shape reward is less than 0.5 and the SNR for the fuel rewards is less than 0.02, diluting nearly the entirety of the reward signal. Further evidence about the noise-robustness of different pruning strengths is provided in Section A.1.

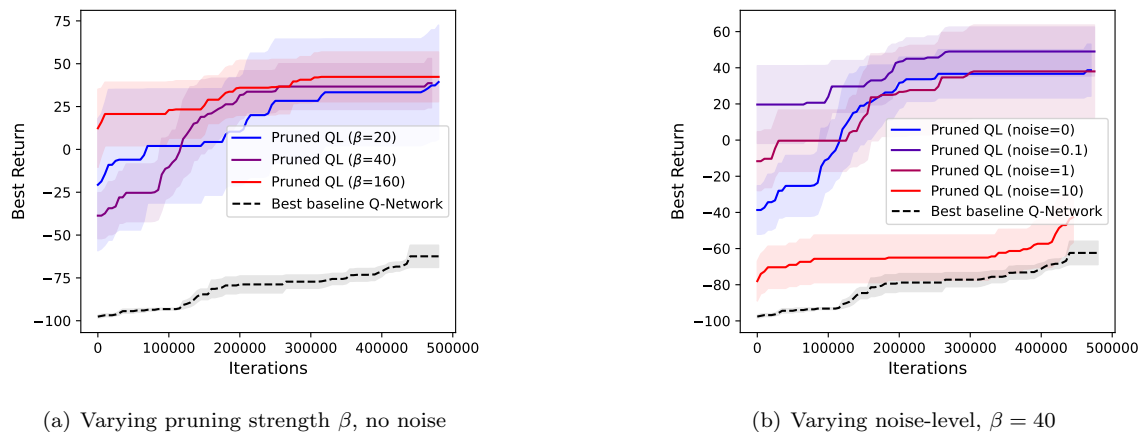


Figure 1: Learning curves indicating policy performance of Pruned QL vs. best baseline Q-Network under (a) different pruning strength, and (b) varying noise level.

Model Parameters. In both experiments on Lunar Lander we used similar parameters. We used a Dirichlet distribution with parameter 10 as the prior over the weighting of rewards.³ We did not discount future rewards ($\gamma = 1$). The Q-function is implemented as a 3-layer feed-forward neural network with ReLU activation. We used the Adam optimizer with a learning rate of 10^{-4} . The frequency of updating the target network is once every 3000 updates of the Q-network. Please refer to the accompanying code for the remaining Q-learning parameters.

²Unless otherwise stated, we use double Q-learning in all experiments.

³We chose a Dirichlet distribution as our prior because it is flexible, intuitive, and often the first choice for modeling nonnegative variables that sum to one, like probabilities. Our results are not sensitive to this parameter choice as long as the chosen prior is not very spread-out or very concentrated.

5.2 Real-World Data Experiments on MIMIC-III

5.2.1 Cohort and Study Design

We evaluate our framework in a real-life offline learning setting by training and evaluating policies for the management of vasopressor and intravenous (IV) fluids in septic patients at intensive care units (ICU). Existing work (Komorowski et al., 2018; Peng et al., 2018; Fatemi, Killian, et al., 2021) in this area has mainly focused on reward specifications based on 90-day mortality. In contrast, we investigate whether Pruned CQL can facilitate learning superior policies by incorporating information from intermediate severity proxies such as the SOFA score (Vincent et al., 1996) and the patient’s lactate level.

Data. We will use data from a cohort of septic ICU patients in the MIMIC-III dataset. This dataset consists of deidentified electronic health records of over 40,000 patients that were admitted to the critical care units of the Beth Israel Deaconess Medical Center in Boston between 2001 and 2012. To construct our sample, we followed the preprocessing steps applied in Komorowski et al. (2018). We excluded patients younger than 18 years old at ICU admission or where mortality and intravenous fluid intake have not been documented. A trajectory includes data from 24 hours before the sepsis onset up until 48 hours after the onset, recorded in 4-hour intervals. For every trajectory, we extracted a set of 48 variables, including demographics, Elixhauser comorbidity index (Elixhauser et al., 1998), vital signs, laboratory test results, and medication dosing decisions. All models are trained on 80% of the data, validated on 5%, and tested on 15% for the final evaluation.

Action Set and State Space. Following previous work by Komorowski et al. (2018) and Fatemi, Killian, et al. (2021), we discretize actions into 25 treatment choices (5 discrete levels for IV fluids and 5 discrete levels for vasopressor dosage). To derive the state space, we applied K-means clustering to the 44-dimensional features and obtained 752 clusters. As the resulting cluster indicators were not numerically meaningful, we additionally applied the continuous bag of words method (Mikolov et al., 2013) to the patients’ state trajectories. This provided us with a 13-dimensional representation for each cluster. Thus, our problem formulation is based on a 25-dimensional action space and a 13-dimensional state space. The resulting dataset consists of 20,912 ICU stay trajectories, of which 4,917 resulted in patient death within 90 days of the patient’s critical care visit.

Reward Specification. We assign a reward of 100 to the final state of a trajectory if the patient survives for at least 90 days past ICU admission, and a reward of -100 otherwise. Achieving a low 90-day mortality is the ultimate goal of our learning agent but since this is a sparse and delayed signal, we further include four medically-motivated rewards that are observed more frequently throughout the patient’s stay:

- **One-period SOFA score change:** The negative of the one-period change in SOFA score.
- **Two-period SOFA score change:** The negative of the two-period change in SOFA score.
- **One-period lactate level change:** The negative of the one-period change in the lactate level.
- **Two-period lactate level change:** The negative of the two-period change in the lactate level.

SOFA (Vincent et al., 1996) is a medical risk score that summarizes the extent of a patient’s organ failure and in recent years has become a key indicator of the sepsis syndrome (Lambden et al., 2019). Arterial lactate levels are an important biomarker for septic shock because they are closely associated with cellular hypoxia. Sepsis can cause an imbalance in oxygen supply and demand, resulting in inadequate delivery of oxygen to the cells and tissues. This can lead to anaerobic metabolism and the production of lactate as a byproduct. Increased arterial lactate levels, therefore, indicate that there is a mismatch between oxygen supply and demand and that the body is experiencing hypoxia (Gernardin et al., 1996). Reward values are scaled to have a standard deviation of one before feeding to the algorithms.

Model Parameters. In this offline RL setting, we employ Pruned CQL with a conservativity level of $\alpha = 0.001$ in all experiments. As the trajectories tend to be short in this setting, we do not discount future rewards ($\gamma = 1$). The Q-function is implemented as a 3-layer feed-forward neural network with ReLU activation. We used a Dirichlet distribution with parameter 10 as the prior \mathcal{P} but results are not sensitive to this choice as long as the prior is not very broad or very concentrated. We treated β as a hyperparameter that takes a value from 20, 40, or 160. We used the Adam optimizer with a learning rate of 10^{-5} in the first phase and 10^{-4} in the second phase. The target network is updated after every 1000 and 8000 updates of the Q-network in the first and second phases, respectively. The baseline model employs the same parameters as the second-phase model. Please refer to the accompanying code for the remaining Q-learning parameters.

5.2.2 Policy Evaluation Approach

In the offline RL setting, it is not feasible to roll out the learned policies and observe their returns. Therefore, we will evaluate the policies using weighted importance sampling. Additionally, we will use a descriptive measure to assess whether the learned Q-functions are capable of distinguishing between high and low mortality trajectories.

There are several approaches to estimating policy values in offline settings, each with its own limitations. Interested readers may refer to Tang and Wiens (2021) for an empirical comparison of different methods and Gottesman et al. (2018) for practical considerations. One effective class of methods for policy evaluation in the offline setting is the class of importance sampling methods, which estimate the policy value by re-weighting trajectories based on their relative likelihood of occurring. However, this requires having a stochastic policy and knowledge of the physician’s policy. To accommodate our final phase 2 deterministic policy, we thus follow the recommendation of Tang, Modi, M. W. Sjoding, et al. (2020) and soften our policy: $\tilde{\pi}(a|s) = (1 - \epsilon)\mathbb{1}\{a = \pi(s)\} + \frac{\epsilon}{|\mathcal{A}|-1}\mathbb{1}\{a \neq \pi(s)\}$. Here π and $\tilde{\pi}$ are the original deterministic policies and the softened version, respectively, and ϵ is a hyperparameter set to $\epsilon = 0.01$. To calculate the importance ratio, we approximate the physician’s policy with a stochastic policy by training a multi-class logistic regression with cross-entropy loss. We then implement the weighted importance sampling (WIS) method to estimate policy values as it has a lower variance than ordinary importance sampling methods. Detailed information on the formulation of WIS can be found in Gottesman et al. (2018) and Tang and Wiens (2021).

One drawback of the WIS estimator is that it is biased toward the behavioral policy. Hence we further analyze a descriptive measure to provide a supplemental perspective to the established off-policy evaluation WIS. Specifically, we aim to evaluate the capability of our Q-function Q to differentiate between trajectories that resulted in patient survival compared to those that led to patient death. This is relevant since a high capacity of a Q-function to distinguish between low and high-risk state-action pairs increases our confidence that choosing the actions with the highest predicted Q-value is beneficial. We adopt the following approach to estimate such a descriptive measure. Consider a trajectory τ from the test data and let r_*^τ be the mortality-based reward assigned to its final state. As noted above, $r_*^\tau = 100$ if the patient survives and $r_*^\tau = -100$ otherwise. We compute $Q(s, a)$ for each state-action pair $(s, a) \in \tau$. Note that $Q(s, a)$ is supposed to be the expected return from the optimal policy at state s followed by action a and not the return of the physician’s policy r_*^τ . But if the optimal policy is sufficiently similar to the physicians, $Q(s, a)$ shall reflect r_*^τ , and we would like to see a larger $Q(s, a)$ if τ results in the patient survival. To measure this association, we bin the Q-values into quartiles and calculate the mortality rate in the lower quartile range $MR(Q_1)$ and the mortality rate in the upper quartile range $MR(Q_3)$. We then report the difference $\Delta MR = MR(Q_1) - MR(Q_3)$. A larger ΔMR indicates that the policy is more effective in distinguishing survival from death trajectories.

5.2.3 Policy Evaluation Results

We first observe that directly incorporating rewards based on the SOFA score and arterial lactate level does not improve performance. In fact, testing a range of relative weights, we found that the policies that performed the best were those that assigned the lowest weight to the intermediate rewards. This observation suggests that directly including intermediate signals may lead to more challenges than benefits in this setting. We further discuss this phenomenon and potential explanations for it in Section B.1.

We next evaluate whether our two-stage Pruned CQL algorithm can leverage the additional information provided by the intermediate rewards to achieve a better ΔMR and higher policy value estimated by WIS.

Table 1: Comparison of different methods in terms of ΔMR , WIS-based policy value, and percentage of actions taken by the policy that match the physician’s actions. Standard errors are calculated based on ten random seeds. The behavior policy has a return of 51.9.

Model	ΔMR (%)	Value (WIS)	Similarity to physicians (%)
CQL($\alpha = 0.001$)	24.6 ± 1.0	14 ± 18	10.4 ± 0.7
CQL($\alpha = 0.005$)	23.6 ± 1.0	35 ± 21	18.6 ± 0.6
CQL($\alpha = 0.01$)	22.6 ± 0.9	26 ± 25	26.2 ± 1.0
Pruned CQL($\alpha = 0.001, \beta = 20$)	24.5 ± 0.9	32 ± 12	11.3 ± 1.2
Pruned CQL($\alpha = 0.001, \beta = 40$)	<u>25.2 ± 0.6</u>	41 ± 15	15.6 ± 0.9
Pruned CQL($\alpha = 0.001, \beta = 160$)	24.2 ± 1.1	<u>66 ± 19</u>	22.1 ± 0.9

The results of our evaluation are summarized in Table 1. We note four key observations from our results. First, Pruned CQL often achieves better ΔMR and WIS values compared to CQL, indicating that our two-stage strategy has been effective in extracting information from the intermediate rewards. Second, Pruned CQL with $\beta = 160$ is superior to the physician’s policy with the observed value of 51.9. Since WIS is conservative in nature, this is an encouraging performance for the obtained policy. The standard CQL method does not show such promise. Third, one potential concern regarding action pruning is that it may eliminate important options from the action space. However, even when we perform strong pruning with $\beta = 160$, the performance of the final policy is not substantially affected, and in fact, the final policies became more similar to those of the physicians, suggesting that the pruning procedure primarily removed less relevant actions. Last but not least, our method often suffers from less variance, here measured across 10 random seeds, which offers higher reliability.

Furthermore, Table 1 demonstrates that more stringent pruning leads to policies that are more similar to those of physicians. This is expected, as stricter pruning corresponds to a greater reliance on intermediate severity indicators, which are important in the physician’s workflow. Similarly, as expected a higher value of the conservativity α results in a greater agreement between the CQL policies and the actions taken by physicians. Notably, however, at similar levels of agreement with the actions taken by physicians, the Pruned CQL policy outperforms the baseline CQL policy in terms of ΔMR and policy value. This effect is also evident in Figure 2, where we have plotted ΔMR and the WIS value against the similarity to physician actions. The different points on the figure correspond to varying levels of α and β . Different trends for ΔMR and WIS-based value might origin from the fact that WIS is biased towards policies more similar to the behavior policy. The results indicate that pruning is more effective than a standard conservative loss in learning effective RL policies while enforcing closeness to the behavior policy. Overall, this recommends action pruning as a promising avenue for incorporating human guidelines into policy optimization.

To further analyze the Q-values obtained from pruned CQL we calculated Q-values for each state-action pair in the test data and divided them into 25 bins. For each bin, we calculated the probability of patient survival. Figure 3 presents the survival rate per bin for pruned CQL with a conservativity level of $\alpha = 0.001$ and pruning strictness of $\beta = 40$. The plot shows a strong positive relationship, indicating a survival rate below 30% for state-action pairs with the lowest Q-values and of over 80% for trajectories with the highest Q-values. These results suggest that the Pruned CQL policy is based on a Q-function that effectively distinguishes high- and low-risk state-action pairs, which is crucial for identifying relevant policies. In Section B.2 we demonstrate similar results for pruning strictness levels of $\beta = 20, 160$.

5.2.4 Pruning Analysis

In order to evaluate our pruning quality, we investigate two key questions: 1) Does our pruning procedure in phase 1 allow us to significantly reduce the size of the action space? 2) Is the resulting action space consistent with current medical practice?

Table 2 presents the average number of available actions after pruning and the corresponding recall of these action sets. As there is no ground truth best policy available, we define recall based on whether the pruned action sets contain the physician actions taken in each respective state in the test set. Since

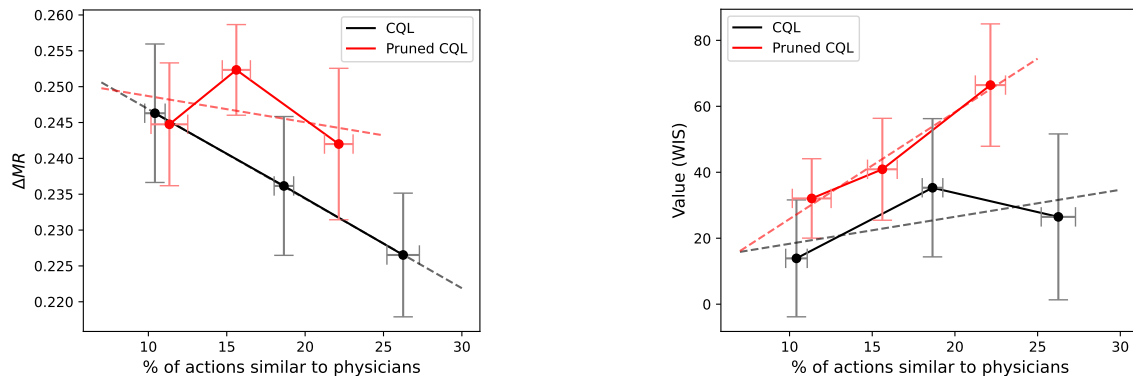


Figure 2: Comparison of Pruned CQL and CQL in terms of ΔMR , WIS-based policy value, for different degrees of overlap with the behavior policy. Dashed lines correspond to linear fits.

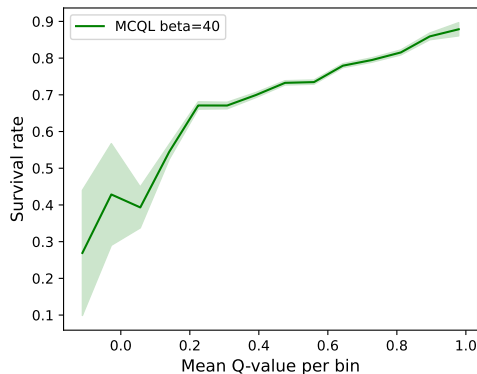


Figure 3: Survival rate by Q-value. Rate plotted for 25 equal-sized bins.

physicians are highly trained professionals and may have access to additional indicators not captured in our records, we aim to retain their decisions among the available options as much as possible. We observe that our pruning procedure significantly reduces the size of the original 25-dimensional action space. Moderate pruning with $\beta = 40$ reduces the mean action set size to less than half, while stricter pruning with $\beta = 160$ reduces the average number of available actions to almost one-sixth. However, even with such aggressive pruning, our method manages to maintain a high recall, ranging from 50% to above 90%, well beyond the chance level.

Table 2: Mean action set size and recall for different pruning levels. The initial action set size was 25.

β	Num. of available actions after pruning	Recall (%)
20	19.7 ± 0.3	94.7 ± 0.3
40	11.6 ± 0.7	83.3 ± 1.4
160	4.1 ± 0.3	49.4 ± 1.9

To investigate the pruning behavior further, Figure 4 displays the distribution of removed actions compared to the actions taken by physicians in the test set for $\beta = 40$. A similar observation holds for less or more strict pruning levels, as described in Section B.3. The figure suggests that our procedure primarily prunes extreme dosing regimes or incoherent decisions, such as a low intravenous fluid dose, while assigning

a high vasopressor dose. These insights further support the idea that the pruning procedure reduces the complexity of the RL problem while retaining relevant actions for the second learning stage.

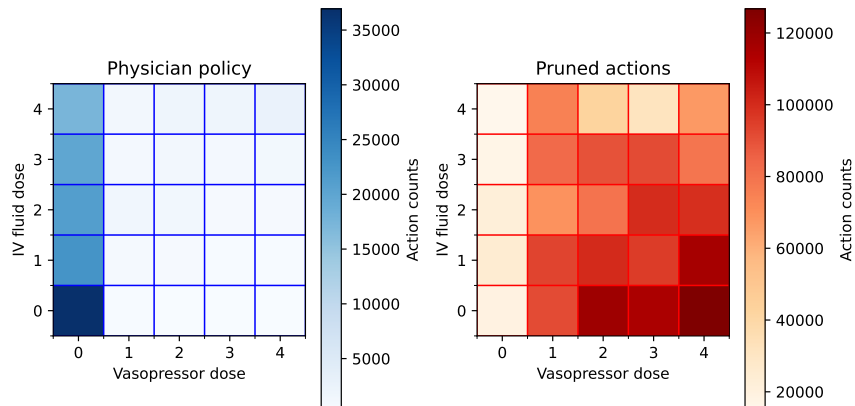


Figure 4: Distribution of observed physician actions and pruned actions ($\beta=40$).

6 Discussion

In this study, we have introduced a novel reinforcement learning method that utilizes action space pruning to facilitate learning when the main reward signal is sparse, intermediate signals are approximate, and there is ambiguity about the weights that should be given to optimal reward components. Our work introduces new algorithms in order to effectively integrate more frequent but imprecise reward proxies into learning.

We demonstrate in the off-policy setting of the Lunar Lander environment that action-space pruning enables Q-learning from the sparse reward alone when standard Q-learning approaches fail. Furthermore, in an offline setting aiming to design vasopressor and intravenous fluid dosing policies for septic patients in the ICU, our results indicate the effectiveness of the pruning approach to reduce the size of the action space while preserving relevant actions. Our trained policy behaves safely by staying mostly consistent with the physician’s policy while achieving better performance than a conservative Q-learning policy for the same level of agreement with the physician’s actions. These results indicate that our learning framework facilitates the efficient incorporation of recurrent yet imprecise reward signals while preventing such signals from causing the policy to diverge from maximizing the primary sparse reward of interest.

Though motivated by the healthcare setting our approach is applicable to further domains in which the true reward signal of interest is sparse and available proxies are frequent but only provide imperfect indicators of the ultimate outcome.

Limitations. While our study provides valuable insights, it has some limitations. First, our results are based on data up to the year 2012, and sepsis treatment guidelines have been evolving since then. Hence, the estimated physician policies in this work may reflect a slightly outdated standard of care. Second, our method relies on the availability of intermediate reward signals that can serve as proxies for the final outcome of interest. In cases where such meaningful signals are not available, our method may not be applicable. Finally, in this study, we have utilized weighted importance sampling (WIS) as an off-policy evaluation method. Although it is a widely accepted technique for evaluating RL policies in offline settings, it is also known to have high variance and is dependent on accurate estimation of the behavior policy (Tang and Wiens, 2021). We partially addressed this issue by evaluating our policy using a related descriptive measure that highlights consistent results with the provided WIS estimates.

References

- Barrett, Leon and Srinu Narayanan (2008). “Learning all optimal policies with multiple criteria”. In: *Proceedings of the 25th international conference on Machine learning - ICML '08*. DOI: [10.1145/1390156.1390162](https://doi.org/10.1145/1390156.1390162). URL: <http://dx.doi.org/10.1145/1390156.1390162>.
- Brockman, Greg et al. (2016). *OpenAI Gym*. eprint: [arXiv:1606.01540](https://arxiv.org/abs/1606.01540).
- Cheng, Li-Fang, Niranjani Prasad, and Barbara E Engelhardt (2018a). “An optimal policy for patient laboratory tests in intensive care units”. In: *BIOCOMPUTING 2019: Proceedings of the Pacific Symposium*. World Scientific, pp. 320–331.
- (Nov. 2018b). “An Optimal Policy for Patient Laboratory Tests in Intensive Care Units”. In: *Biocomputing 2019*. DOI: [10.1142/9789813279827_{_}0029](https://doi.org/10.1142/9789813279827_{_}0029). URL: http://dx.doi.org/10.1142/9789813279827_0029.
- Elixhauser, Anne et al. (1998). “Comorbidity measures for use with administrative data”. In: *Medical care*, pp. 8–27.
- Fard, M Milani and Joelle Pineau (2011). “Non-deterministic policies in Markovian decision processes”. In: *Journal of Artificial Intelligence Research* 40, pp. 1–24.
- Fatemi, Mehdi, Taylor W Killian, et al. (2021). “Medical Dead-ends and Learning to Identify High-risk States and Treatments”. In: *Advances in Neural Information Processing Systems* 34, pp. 4856–4870.
- Fatemi, Mehdi, Shikhar Sharma, et al. (May 2019). “Dead-ends and Secure Exploration in Reinforcement Learning”. In: *International Conference on Machine Learning* 97, pp. 1873–1881. URL: <http://proceedings.mlr.press/v97/fatemi19a/fatemi19a.pdf>.
- Futoma, Joseph et al. (Aug. 2017). “An Improved Multi-Output Gaussian Process RNN with Real-Time Validation for Early Sepsis Detection”. In: *arXiv: Machine Learning*. URL: <https://arxiv.org/pdf/1708.05894.pdf>.
- Gernardin, G et al. (1996). “Blood pressure and arterial lactate level are early indicators of short-term survival in human septic shock”. In: *Intensive care medicine* 22, pp. 17–25.
- Gottesman, Omer et al. (2018). “Evaluating reinforcement learning algorithms in observational health settings”. In: *arXiv preprint arXiv:1805.12298*.
- Henry, Katharine E et al. (2015). “A targeted real-time early warning score (TREWScore) for septic shock”. In: *Science translational medicine* 7.299, 299ra122–299ra122.
- Hiraoka, Kazuyuki, Manabu Yoshida, and Taketoshi Mishima (Oct. 2008). “Parallel reinforcement learning for weighted multi-criteria model with adaptive margin”. In: *Cognitive Neurodynamics* 3.1, pp. 17–24. DOI: [10.1007/s11571-008-9066-9](https://doi.org/10.1007/s11571-008-9066-9). URL: <http://dx.doi.org/10.1007/s11571-008-9066-9>.
- Iima, Hitoshi and Yasuaki Kuroe (Oct. 2014). “Multi-objective reinforcement learning for acquiring all Pareto optimal policies simultaneously - Method of determining scalarization weights”. In: *2014 IEEE International Conference on Systems, Man, and Cybernetics (SMC)*. DOI: [10.1109/smc.2014.6974022](https://doi.org/10.1109/smc.2014.6974022). URL: <http://dx.doi.org/10.1109/smc.2014.6974022>.
- Irpan, Alex et al. (Dec. 2018). “Off-Policy Evaluation via Off-Policy Classification”. In: *Neural Information Processing Systems* 32, pp. 5437–5448. URL: <https://arxiv.org/pdf/1906.01624.pdf>.
- Johnson, Alistair EW et al. (2016). “MIMIC-III, a freely accessible critical care database”. In: *Scientific data* 3.1, pp. 1–9.
- Komorowski, Matthieu et al. (2018). “The artificial intelligence clinician learns optimal treatment strategies for sepsis in intensive care”. In: *Nature medicine* 24.11, pp. 1716–1720.
- Kumar, Aviral et al. (2020). “Conservative q-learning for offline reinforcement learning”. In: *Advances in Neural Information Processing Systems* 33, pp. 1179–1191.
- Lambden, Simon et al. (2019). “The SOFA score—development, utility and challenges of accurate assessment in clinical trials”. In: *Critical Care* 23.1, pp. 1–9.
- Lin, Rongmei et al. (July 2018). “A Deep Deterministic Policy Gradient Approach to Medication Dosing and Surveillance in the ICU”. In: *2018 40th Annual International Conference of the IEEE Engineering in Medicine and Biology Society (EMBC)*. DOI: [10.1109/embc.2018.8513203](https://doi.org/10.1109/embc.2018.8513203). URL: <http://dx.doi.org/10.1109/embc.2018.8513203>.
- Liu, Chunming, Xin Xu, and Dewen Hu (Mar. 2015). “Multiobjective Reinforcement Learning: A Comprehensive Overview”. In: *IEEE Transactions on Systems, Man, and Cybernetics: Systems* 45.3, pp. 385–398. DOI: [10.1109/tsmc.2014.2358639](https://doi.org/10.1109/tsmc.2014.2358639). URL: <http://dx.doi.org/10.1109/tsmc.2014.2358639>.

- Liu, Siqi et al. (July 2020). “Reinforcement Learning for Clinical Decision Support in Critical Care: Comprehensive Review”. In: *Journal of Medical Internet Research* 22.7, e18477. DOI: [10.2196/18477](https://doi.org/10.2196/18477). URL: <http://dx.doi.org/10.2196/18477>.
- Lizotte, Daniel J and Eric B Laber (2016). “Multi-objective Markov decision processes for data-driven decision support”. In: *The Journal of Machine Learning Research* 17.1, pp. 7378–7405.
- Mannor, Shie and Nahum Shimkin (Jan. 2001). “The Steering Approach for Multi-Criteria Reinforcement Learning”. In: *Neural Information Processing Systems* 14, pp. 1563–1570.
- Mikolov, Tomas et al. (2013). “Efficient estimation of word representations in vector space”. In: *arXiv preprint arXiv:1301.3781*.
- Miller, William Dwight et al. (2021). “Accuracy of the sequential organ failure assessment score for in-hospital mortality by race and relevance to crisis standards of care”. In: *JAMA network open* 4.6, e2113891–e2113891.
- Mossalam, Hossam et al. (Oct. 2016). “Multi-Objective Deep Reinforcement Learning”. In: *arXiv: Artificial Intelligence*. URL: <https://arxiv.org/pdf/1610.02707.pdf>.
- Natarajan, Srimaam and Prasad Tadepalli (2005). “Dynamic preferences in multi-criteria reinforcement learning”. en. In: *Proceedings of the 22nd international conference on Machine learning - ICML '05*. Bonn, Germany: ACM Press, pp. 601–608. ISBN: 9781595931801. DOI: [10.1145/1102351.1102427](https://doi.org/10.1145/1102351.1102427). URL: <http://portal.acm.org/citation.cfm?doid=1102351.1102427> (visited on 01/20/2023).
- Peine, Arne et al. (Feb. 2021). “Development and validation of a reinforcement learning algorithm to dynamically optimize mechanical ventilation in critical care”. In: *npj Digital Medicine* 4.1. DOI: [10.1038/s41746-021-00388-6](https://doi.org/10.1038/s41746-021-00388-6). URL: <http://dx.doi.org/10.1038/s41746-021-00388-6>.
- Peng, Xuefeng et al. (Dec. 2018). “Improving Sepsis Treatment Strategies by Combining Deep and Kernel-Based Reinforcement Learning.” In: *American Medical Informatics Association Annual Symposium* 2018, pp. 887–896.
- Prasad, Niranjani et al. (Apr. 2017). “A Reinforcement Learning Approach to Weaning of Mechanical Ventilation in Intensive Care Units”. In: *arXiv: Artificial Intelligence*. URL: <https://arxiv.org/pdf/1704.06300.pdf>.
- Raghu, Aniruddh, Matthieu Komorowski, Leo Anthony Celi, et al. (2017). “Continuous state-space models for optimal sepsis treatment: a deep reinforcement learning approach”. In: *Machine Learning for Healthcare Conference*. PMLR, pp. 147–163.
- Raghu, Aniruddh, Matthieu Komorowski, and Sumeetpal Singh (2018). “Model-based reinforcement learning for sepsis treatment”. In: *arXiv preprint arXiv:1811.09602*.
- Saria, Suchi (Nov. 2018). “Individualized sepsis treatment using reinforcement learning”. In: *Nature Medicine* 24.11, pp. 1641–1642. DOI: [10.1038/s41591-018-0253-x](https://doi.org/10.1038/s41591-018-0253-x). URL: <http://dx.doi.org/10.1038/s41591-018-0253-x>.
- Song, Zhao, Ron Parr, and Lawrence Carin (2019). “Revisiting the softmax bellman operator: New benefits and new perspective”. In: *International conference on machine learning*. PMLR, pp. 5916–5925.
- Tang, Shengpu, Aditya Modi, Michael Sjoding, et al. (2020). “Clinician-in-the-loop decision making: Reinforcement learning with near-optimal set-valued policies”. In: *International Conference on Machine Learning*. PMLR, pp. 9387–9396.
- Tang, Shengpu, Aditya Modi, Michael W. Sjoding, et al. (July 2020). “Clinician-in-the-Loop Decision Making: Reinforcement Learning with Near-Optimal Set-Valued Policies”. In: *International Conference on Machine Learning* 1, pp. 9387–9396. URL: <http://proceedings.mlr.press/v119/tang20c/tang20c.pdf>.
- Tang, Shengpu and Jenna Wiens (2021). “Model selection for offline reinforcement learning: Practical considerations for healthcare settings”. In: *Machine Learning for Healthcare Conference*. PMLR, pp. 2–35.
- Tesauro, Gerald et al. (Dec. 2007). “Managing Power Consumption and Performance of Computing Systems Using Reinforcement Learning”. In: *Neural Information Processing Systems* 20, pp. 1497–1504. URL: http://lass.cs.umass.edu/~shenoy/courses/fall09/691gc/papers/Kephart-2007-1-NIPS2007_0906.pdf.
- Van Hasselt, Hado, Arthur Guez, and David Silver (2016). “Deep reinforcement learning with double q-learning”. In: *Proceedings of the AAAI conference on artificial intelligence*. Vol. 30.
- Van Moffaert, Kristof, Madalina M. Drugan, and Ann Nowe (Apr. 2013). “Scalarized multi-objective reinforcement learning: Novel design techniques”. In: *2013 IEEE Symposium on Adaptive Dynamic Pro-*

- gramming and Reinforcement Learning (ADPRL)*. DOI: [10.1109/adprl.2013.6615007](https://doi.org/10.1109/adprl.2013.6615007). URL: <http://dx.doi.org/10.1109/adprl.2013.6615007>.
- Vincent, J. -L. et al. (July 1996). “The SOFA (Sepsis-related Organ Failure Assessment) score to describe organ dysfunction/failure”. In: *Intensive Care Medicine* 22.7, pp. 707–710. ISSN: 1432-1238. DOI: [10.1007/BF01709751](https://doi.org/10.1007/BF01709751). URL: <https://doi.org/10.1007/BF01709751>.
- Xu, Jie et al. (July 2020). “Prediction-Guided Multi-Objective Reinforcement Learning for Continuous Robot Control”. In: *International Conference on Machine Learning* 1, pp. 10607–10616. URL: <http://proceedings.mlr.press/v119/xu20h/xu20h.pdf>.

A Further Insights From LunarLander Experiments

A.1 Robustness to Noise

To augment the findings illustrated in Figure 1, we depict the effect of noise on Pruned QL performance in for $\beta = 20, 160$ in Figure 5. Overall, the main results discussed continue to hold, Pruned QL behaves robustly to the noise until raising the noise standard deviation to 10.

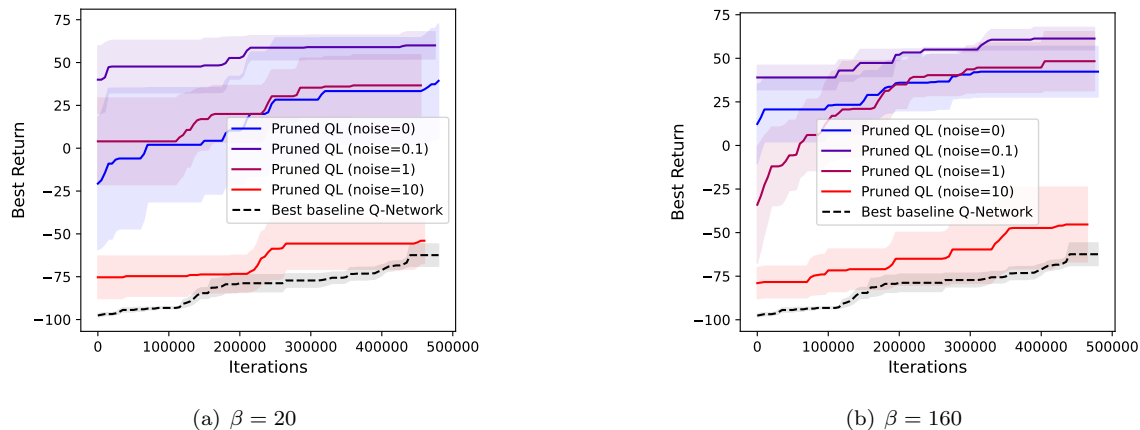


Figure 5: Learning curves indicating policy performance of Pruned QL vs. best baseline Q-Network under different noise levels.

B Further Insights From MIMIC-III Experiments

B.1 Learning From Individual Rewards

We run standard Q-learning on each individual reward. Figure 6(a) shows learning during training with different settings. The learning rate of 10^{-4} and target network update frequency (TUF) of 8000 are the optimal choice of parameters to learn from the sparse reward. However, as the figure suggests, learning from intermediate rewards like SOFA-1 and LAC-1 requires a slower learning rate and decreased TUF. Further, the optimal choice of the number of iterations before overfitting also differs for two types of reward. Another way to see this is in Figure 6(b) where we have plotted the best ΔMR for each setting. One can see that changing the learning rate and TUF has opposite effects on Q-learning from the sparse reward and Q-learning from intermediate rewards. This observation can explain why linearly mixing sparse and intermediate rewards might not be a good idea.

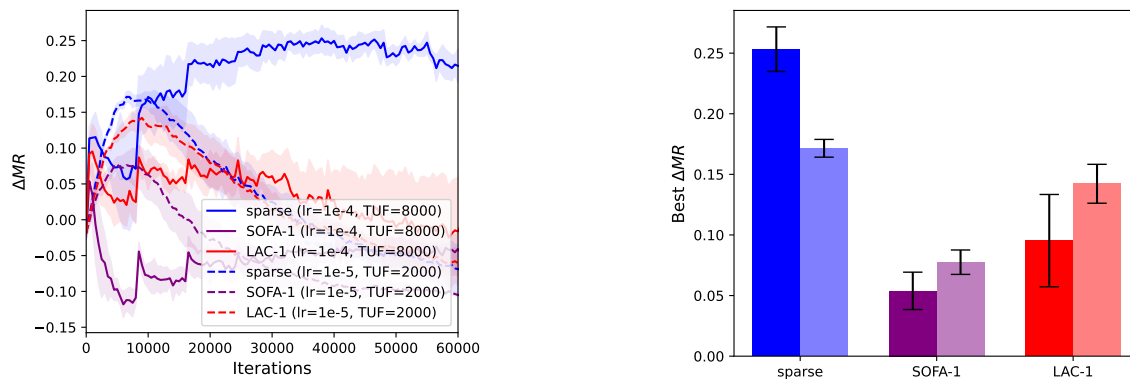


Figure 6: Running Q-learning based on different rewards and settings. The learning curves show intermediate rewards require a slower learning rate and lower target update frequency. The bar plot shows the best ΔMR in each setting. The darker bars correspond to the learning rate of 10^{-4} and TUF of 8000.

B.2 Survival Rate Versus Q-Value for Different Pruning Strengths

To augment the findings illustrated in Figure 3, we depict the survival curve for pruning strength $\beta = 20, 160$ in Figure 7.

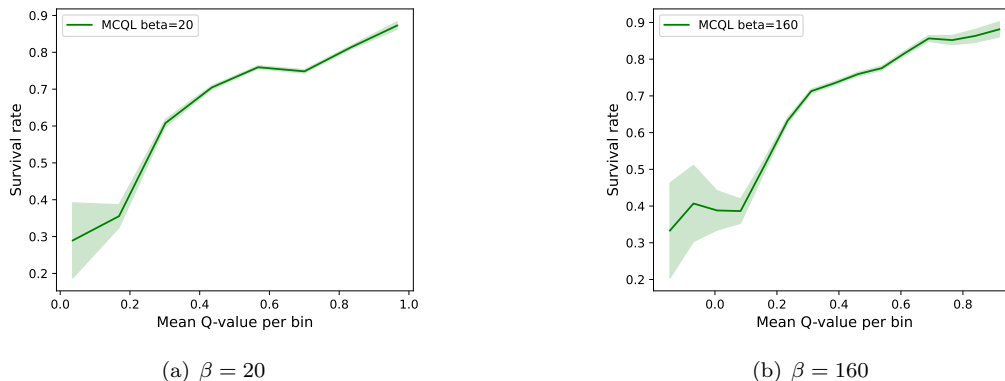


Figure 7: Relationship between Q-values and patient survival for different β .

B.3 Pruning for Different Pruning Strengths

To augment the findings illustrated in Figure 4, we depict the effect of pruning strength on the distribution of removed actions in Figure 8 for $\beta = 20, 160$.

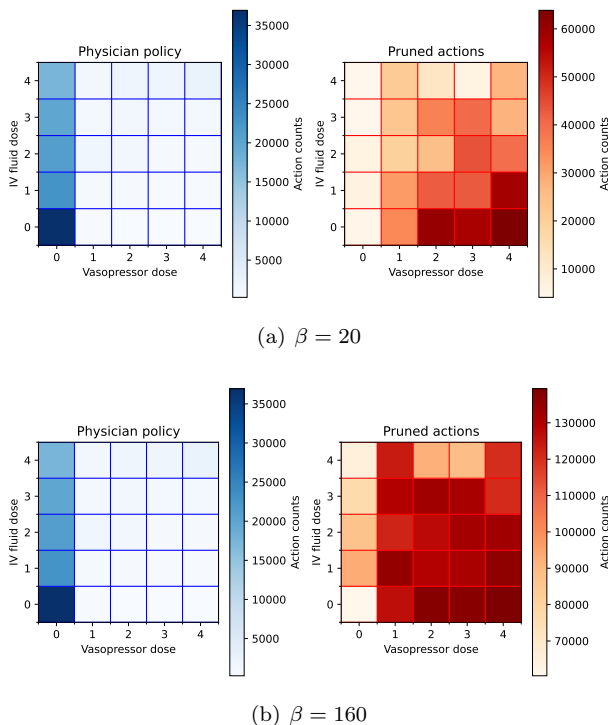


Figure 8: Distribution of pruned actions for different pruning strengths.